Case Studies in Construction Materials 18 (2023) e01913

Contents lists available at ScienceDirect

Case Studies in Construction Materials

journal homepage: www.elsevier.com/locate/cscm

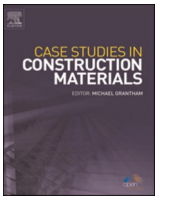

Case study

Deterministic and probabilistic approaches for corrosion in RC structures: A direct proposed model to total service life predictions

Caio Gorla Nogueira [a,*], Lucas Yoshio [a], Enrico Zacchei [b,c,**]

[a] School of Civil Engineering, São Paulo State University (UNESP), 14-01 Eng. Luís Edmundo Carrijo Coube Avenue, 17033-360, Bauru-SP, Brazil
[b] Itecons, Coimbra, Portugal
[c] University of Coimbra, CERIS, Coimbra, Portugal

ARTICLE INFO

Keywords:
Chloride diffusion
Pitting corrosion
Reliability analysis
Resistance losses
Risk analysis
Total time of service life

ABSTRACT

In this paper the negative effects of the chloride ions attack in reinforced concrete (RC) elements have been studied. For this the vertical and horizontal chloride diffusivity has been treated by several models to identify the more relevant factor affecting the chloride concentration. The pitting corrosion has been treated to define the resistance losses of the shear forces and bending moments. An alternative deterministic/probabilistic procedure, by a direct and systematic new model, has been proposed to estimate the total time of service life for RC elements at the design phase. Several detailing configurations of steel bars in a RC beam, water/cement ratio and level of aggressiveness have been analysed to compare the model predictions. In this sense, this paper should provide useful results for analysts in terms of probability of failure for resistance losses and time of corrosion initiation. The goal is not only to provide practical results but also to evaluate the issue in a more modern risk analysis throughout the proposed prediction model.

1. Introduction

The concepts of service life and structural durability have been extensively explored in the last decades in the engineering area [31, 38, 41]. In the context of reinforced concrete (RC) structures, the prediction of the overall behaviour through its lifetime is mandatory to achieve adequate safety levels and optimize complex costs [4,11,34]. In [54] an interesting current review of the existing studies has been shown focusing on corrosion effects for RC structures.

Environmental actions are the main factors that cause pathological manifestations in RC structures by changing their durability and, consequently, service life of structural systems [1–3,5,10]. However, several RC structures may not indicate visible pathologies especially those related to the corrosion phenomenon.

It is known that the depassivation of steel bars by chloride ions penetration is the most important deterioration mechanism in RC structural elements, affecting their resistant capacity along time [6–9]. There are many factors that influence the chloride concentration thus the corrosion: the proportions and other incorporated materials in the concrete mixture, type of cement, water/cement (w/c) ratio, concrete cover, temperature, humidity, steel surface conditions, external sources of chloride penetration and even loading conditions acting over the structural elements as treated recently in [13,17,37,42].

There are several uncertainties sources associated to many mentioned factors that cannot be neglected when more accurate

* Corresponding author.
** Corresponding author at: Itecons, Coimbra, Portugal.
E-mail addresses: caio.nogueira@unesp.br (C.G. Nogueira), enricozacchei@gmail.com (E. Zacchei).

https://doi.org/10.1016/j.cscm.2023.e01913
Received 30 November 2022; Received in revised form 7 January 2023; Accepted 2 February 2023
Available online 8 February 2023

predictions of durability are needed [12]. In this regard, the assessment of some important parameters, which controls (e.g., time of corrosion initiation) and give information of the status of the corrosion process (e.g., ultimate load capacity), should be done by probabilistic approaches to better predict the durability of RC structures in a more accurate way.

The most of uncertainties can be modelled as random variables as shown in [28,34,53]. Reliability analyses estimate the probability of failure for each considered failure mode, through the uncertainties of the design, environmental and model parameters. Therefore, these probabilistic approaches consider the uncertainties and their effects more consistently, opening a new "layer of information" to better take decisions in engineering projects, especially when the durability aspects are present [28,34].

For this, more innovative approaches try to quantify the weight of each parameter on the chloride diffusion by using, e.g., artificial intelligences [47–50].

The mechanical diffusion of chloride ions into concrete can be modelled by using the Fick's laws, where the diffusion coefficient must be determined [8,10,13,21]. There are several ways to designate this coefficient in function of the w/c ratio, physical properties of cement and aggregate, concentration of free and bonded chlorides, temperature, humidity, effect of concrete aging and external loadings [8,14–17]. In [36], many empirical relations that correlate the diffusion coefficient with these factors have been listed, whereas in [40] a new more complete relation has been proposed.

The abovementioned aspects are related to first phase of the corrosion, whereas the second phase is mainly related to the damage of reinforcements rendering the structure unable to withstand the external applied loadings. Also, corrosion chemical products could have a larger volume than steel, which lead to further development of internal cracks in the concrete. As these cracks develop, the steel-concrete interaction decreases until the breakdown of the concrete cover (i.e., spalling) [19].

Studies in literature [18,20] indicate that when the propagation period begins, structural safety declines in a truly short time due to pitting phenomena (more aggressive with respect uniform corrosion [19]), loss of the cross-section area, internal micro cracks, and spalling. Actually, in [55–57], the pitting phenomenon is also well studied highlighting its negative effect.

In [21] there is a well-known approach to explain the service life of RC structures from the point of view of reinforcement corrosion. However for a real structure this approach appear unsatisfactory for defining the maximum acceptable degree of corrosion. In [43] it was proposed another simplified model where it was treated the definition of the ultimate state that represents the maximum acceptable degree of corrosion.

More recently in [51–53], it was shown how the probabilities of occurrence of certain scenarios, such as the corrosion initiation, corrosion-fatigue damage/crack growth and mechanical failure of a RC member, give more reliable and consistent measures for durability predictions than a single value evaluated by a deterministic approach.

Finally, standard codes [23,32] do not present an explicit mathematical procedure to calculate the total time of service life of RC structures, thus the contribution of this paper is to present a simple model to provide a direct and systematic routine to estimate the total time of service life of RC structures at the design phase.

Therefore, it is extremely important to well model the chloride ingress process and the mechanical resistance loss after pitting corrosion along time. This paper presents an explicit and systematic deterministic-probabilistic approach to estimate the total time of service life applied to RC beams. This study does not present a closed form to perform the total time of service life for RC structures, but it treats all the important aspects to apply the proposed model. Several comparisons between diffusivity models in the initiation phase, as well as deterministic and probabilistic responses in both phases are presented here to provide more suitable experience to use the proposed model.

2. Diffusion mechanical model

2.1. Chloride concentration

The movement of chlorides inside the concrete occurs essentially by diffusion in an aqueous medium, where the moisture percentage is high. Ionic diffusion occurs due to gradients of ionic concentration in the exterior and interior of the concrete. The differences in the chloride concentrations are correlated with their mass balance by Lavoisier's law [3]. Fick's second law (Eq. (1)) considers the variable flow with the penetration depth and time:

$$\frac{\partial C}{\partial t} = \frac{\partial}{\partial x}\left(D_c \frac{\partial C}{\partial x}\right) \tag{1}$$

The adopted assumptions for Eq. (1) are: the material is homogeneous, isotropic and inert, maintaining the same mechanical properties in all directions and over time [21].

The analytical solution of Eq. (1) considers a semi-infinite domain and constant concentration on the structural surface, which is described by [34]:

$$C(x,t) = C_0 \times \left(1 - \mathrm{erf}\left(\frac{x}{2\sqrt{D_c t}}\right)\right) \tag{2}$$

where $C(x,t)$ is the concentration of chloride ions at depth x given a time t, $\mathrm{erf}()$ is the Gaussian error function, and D_c is the apparent diffusion coefficient (here considered constant as explained in Section 2.2). As already mentioned, there are several relations to estimate D_c, e.g., by experimental data [27] or by considering external and internal factors [36].

The parameter C_0 is the concentration of chloride ions on the external surface of the element, and, in this study, it is considered as a

constant over time [45]. From analysed data on ~1158 bridges in Tasmania, in [22] is proposed that C_0 is given as a function of the distance to the coast, d_{cost} (expressed in km). By this study, four levels of environmental aggressiveness have been defined (see Table 1): low, moderate, high, and extreme [19,35].

The corrosion of steel reinforcements starts when a limit concentration, C_{lim} (estimated between 0.60 and 0.90 kg/m^3 in ordinary concrete [9,44]) is reached, affecting the protective passive layer present in the steel. In addition, concrete tends to retain more moisture as the chloride content increases, implying an increase of the corrosion risk in the structure.

2.2. Chloride diffusion coefficient

Here three most used D_c models [14,15,17] were explained to compare the predictions of inner chloride concentration in concrete and to show how it can impact on the total service life of a RC structure in design phase. Bentz et al. [14] and Papardakis et al. [15] consider a constant D_c depending on only concrete characteristics, whereas Fu et al. [17] considers also the temperature and humidity, which implies a time variation of D_c. Just for naming simplification, these models will be called "model B", "model P" and "model F", respectively.

Although model F is more complex than the B and P model, it is considered yet as a simple model present in literature. In fact, the authors of this paper have been developed more advanced models (not treated here) considering dynamic non-linear D_c [13,34,40,45].

2.2.1. Bentz et al. (1996) model [14]

Bentz et al. (1996) [14] has been developed the coefficient D_c, expressed in cm^2/s, by:

$$D_{c,I} = 10^{-10+\left(4.66\times\frac{w}{c}\right)} \tag{3}$$

Eq. (3) has been calibrated by experimental laboratory measurements and it depends on only of w/c ratio. In this sense, the applicability of this relation is very easy; however, it does not account for several factors, e.g., the environmental and load actions.

2.2.2. Papadakis et al. (1996) model [15]

Papadakis et al. (1996) [15] has been proposed a model for D_c (in cm^2/s) that considers the concrete component characteristics, by:

$$D_{c,II} = 0.15 d_{c-H_20} \times \frac{1+\rho_c\left(\frac{w}{c}\right)}{1+\rho_c\left(\frac{w}{c}\right)+\frac{\rho_c}{\rho_{wg}}\left(\frac{w_g}{c}\right)} \times \left(\frac{\rho_c\left(\frac{w}{c}\right)-0.85}{1+\rho_c\left(\frac{w}{c}\right)}\right)^3 \tag{4}$$

where w_g/c is the aggregate mass to the cement mass ratio, ρ_c is the specific mass of the cement, ρ_{ag} is the specific mass of the aggregates, $d_{c\text{-}H20}$ is the diffusion coefficient of chloride in an infinite solution of NaCl given by 1.60×10^{-5} cm^2/s.

2.2.3. Fu et al. (2015) model [17]

This multifactorial model accounts for several factors, including environmental actions (i.e., temporal/climatic variables) on the structures, excepting loadings and damage influence:

$$D_{c,III} = f_{wc} \times f_1(C_b) \times f_2(T) \times f_3(t) \times f_4(h) \tag{5}$$

where f_{wc} is the chloride diffusion constant, referenced in saturated concrete at 28 days, given by $f_{wc} = 10^{-12.06+2.4\left(\frac{w}{c}\right)}$ (expressed in m^2/s).

The factor f_1 is given as a function of the binding concentration C_b, which is correlated to the free concentration C_f and the amount of evaporable water from the concrete ω_e; αandβ are two constant values. The factor f_1 is defined by the Langmuir isotherm model described in [8,16].

The factor f_2 refers to the temperature variation T and it depends on the reference temperature, T_o; the gas universal constant, $\overline{R}$; the activation energy of the diffusion process, E_a, which depends on the cement and the w/c ratio. The factor f_2 is described by Arrhenius' law described in [6,13,24].

The factor f_3, described in [17,25], refers to the effect of concrete aging t, which is correlated to the reference age, t_{ref}; the time when the diffusivity is estimated constant, t_r and the time t of exposure (expressed in years). The index m shows the reduction of the

Table 1
Surface chloride concentration C_0 for environmental aggressiveness [19,35,45].

Level of aggressiveness	Structure description	Average concentration (kg/m^3)
Low	d_{cost} = 2.84 km, or more from the coast.	0.35
Moderate[a]	d_{cost} between 0.10 and 2.84 km from the coast without direct contact with sea water.	1.15
High[a]	d_{cost} less than 0.10 km without direct contact with sea water and thaw salts.	2.95
Extreme	Subject to humidification and drying cycles by sea water.	7.35

[a] In this study the Brazilian code [23] is adopted, where the moderate and high level corresponds to the category II and III of environmental aggressiveness (CAA), respectively.

chloride diffusion speed, which is correlated to the fly ash and slag contained in the concrete.

Finally, the factor f_4 is correlated to the relative humidity of the concrete pores along time, h(t); the humidity at which the coefficient D_c halves between its maximum and minimum values, h_c (according to [26], it remains constant for different concretes and mortars, i.e., $h_c = 0.75$). The factor f_4 is defined by S-shaped curves [8,11].

The h(t) function is expressed in this paper by a sinusoidal trend:

$$h(t) = \frac{h_{max} + h_{min}}{2} + \left[\frac{h_{max} + h_{min}}{2} \times \text{sen}(2\pi(t - 0.5))\right] \quad (6)$$

where h_{max} is the maximum humidity (here assumed $h_{max} = 0.6$) and h_{min} is the minimum humidity (here assumed $h_{min} = 0.8$) [11].

2.3. Comparison between chloride diffusion models

Here some comparisons between three models are shown. All analyses have been performed using w/c = {0.40, 0.50}. The adopted parameters for the f_1, f_2, and f_3 factors in the model F are: $\omega_e = 0.6$; $C_f = 1.50 kg/m^3$; $\alpha = 11.8$; $\beta = 4.0$; $\overline{R} = 8.3145 J/molK$; $T_0 = 296.0K$; $m = 2.0$; $t_{ref} = 28.0 years$; $t_r = 30.0 years$; $T = 293.0K (i.e., \sim 25.0^oC)$. E_a values are 41800.0 J/mol and 44600.0 J/mol for w/c = 0.40 and w/c = 0.50, respectively. The factor f_4 is 0.24 according to the adopted values for h_c, h_{max} and h_{min}. For model P we assume w_g/c, ρ_c, and ρ_{ag} equal to 0.35, 3.0 g/cm^3, and 4.50 g/cm^3, respectively [15]. In Fig. 1, it is possible to see that models B and P provide a constant value for D_c, whereas model F is time variating. Also, D_c is affected by the w/c ratio and, in case of model F, by the $f_3(t)$ factor.

Fig. 2 shows the chloride concentration C at the concrete-steel interface along time for w/c = 0.50. For the class of aggressiveness CAA II and III, the concrete cover x was adopted as 3.0 and 4.0 cm, respectively. The used C_{lim} is 0.60 kg/m^3 since in [44] it is considered a "commonly accepted chloride threshold that facilitates rebar corrosion". Therefore, when C reaches C_{lim} there is an estimative of the time of corrosion initiation. The adopted C_0 values for CAA II and III are 1.15 kg/m^3 and 2.95 kg/m^3, respectively (see Table 1).

The time of corrosion initiation considering all the three models is given by: ~16.0 years (model B), ~9.0 years (model P) and ~37.0 years (model F), in case of CAA II (Fig. 2a)). For CAA III (Fig. 2b)) we obtain: ~7.0 years (model B), ~4.0 years (model P) and ~13.0 years (model F).

Finally, Fig. 3 shows the gradient of chloride concentration C for CAA III and w/c = 0.50. Here, the model F provides the lesser chloride ions concentration along the concrete cover. This is consistent with the diffusivity D_c assessed by this model, which is the lesser value between the two other models.

3. Pitting corrosion model

3.1. Corrosion rate

In [27], it has been proposed an empirical relation, expressed by Eq. (7), to estimate the corrosion rate based on the oxygen diffusion rate, which considers the percentage of the corrosion products and the molecular effects of corrosion in the cathodic zone:

$$i_{corr} = \left[\frac{37.8(1 - w/c)^{-1.64}}{x}\right] 0.85 \times t_p^{-0.29} \quad (7)$$

where i_{corr} is the corrosion rate in μA/cm^2, t_p is the elapsed time referring to the propagation phase (beginning of the corrosive process, expressed in years), x is the cover depth (expressed in cm). In [27], Eq. (7) has been calibrated with constant D_c, h = 75.0%, and T = 20.0 °C since represent the values used in places where it is common to observe corrosion problems in structures.

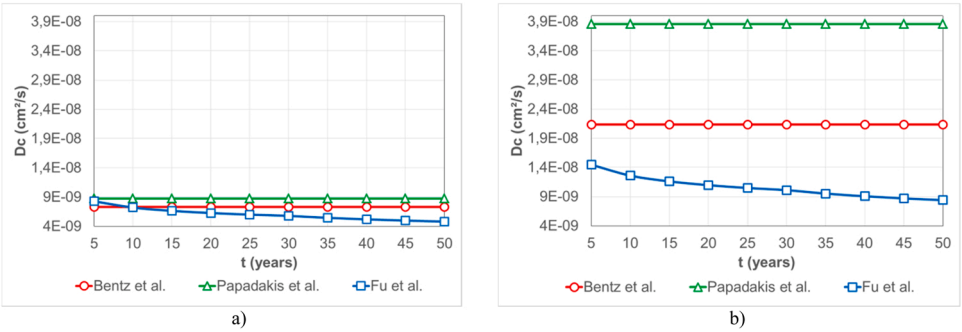

Fig. 1. Comparison of D_c models for w/c = a) 0.40, and b) 0.50.

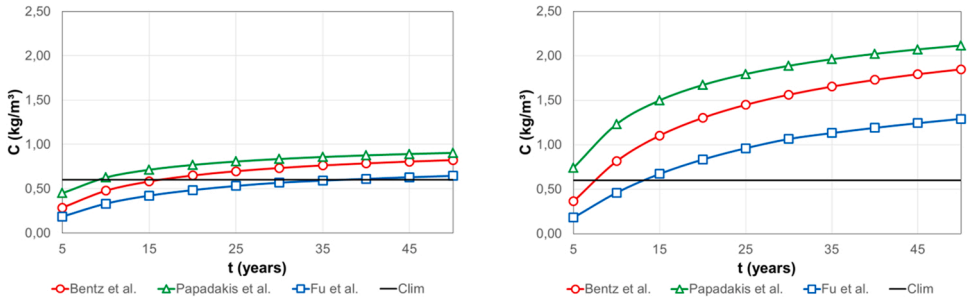

Fig. 2. Chloride concentration for w/c = 0.50: a) CAA II at x = 3.0 cm; b) CAA III at x = 4.0 cm.

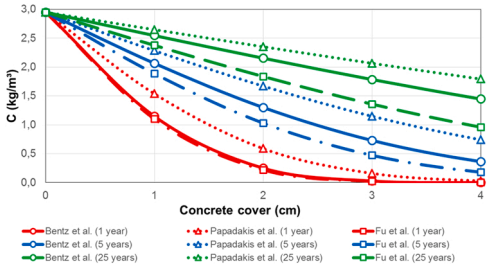

Fig. 3. Chloride concentration for w/c = 0.50 and CAA III (x = 4.0 cm).

3.2. Steel cross-section corroded and residual area

In [19,30], it was presented a way to calculate the residual area of steel bars, $A_{r,pit}$, subjected to pitting corrosion, using Faraday's laws and assuming that the pitting corrosion, A_{pit} (white area) has a spherical shape as shown in Fig. 4.

The radius of the pit, $p(t_p)$, is calculated by [30]:

$$p(t_p) = 0.0116 \times i_{corr} \times \eta \times t_p \tag{8}$$

where η is the pitting factor that represents the ratio between the maximum penetration depth by pit and uniform corrosion.

The depth of the pit, a, and the area of corroded steel A_{pit} in the steel bar are obtained by [27]:

$$a = 2 \times p(t_p)\sqrt{1 - \left[\frac{p(t_p)}{d_0}\right]^2} \tag{9}$$

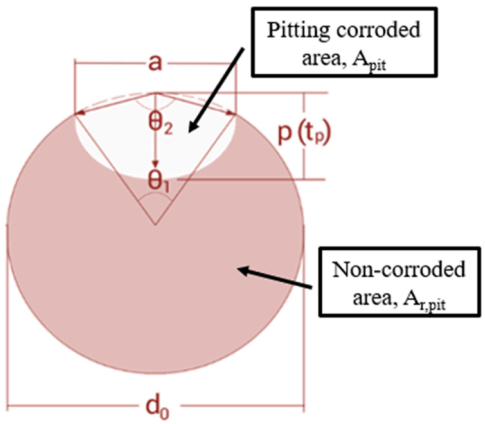

Fig. 4. Pitting configuration of a steel bar (modified from [30]).

$$A_{pit}(t_p) = \begin{cases} A_1 + A_2 & \text{for} : p(t_p) \le \dfrac{d_0}{\sqrt{2}} \\ \dfrac{\pi d_0^2}{4} - A_1 + A_2 & \text{for} : \dfrac{d_0}{\sqrt{2}} < p(t_p) < d_0 \\ \dfrac{\pi d_0^2}{4} & \text{for} : p(t_p) \ge d_0 \end{cases} \quad (10)$$

where d_0 is the diameter of the full steel bar, areas A_1 and A_2 are calculated by, respectively:

$$A_1 = 0.5\left[\theta_1\left(\frac{d_0}{2}\right)^2 - a\left|\frac{d_0}{2} - \frac{p(t_p)^2}{d_0}\right|\right] \quad (11)$$

$$A_2 = 0.5\left[\theta_2 \times p(t_p)^2 - \frac{a \times p(t_p)^2}{d_0}\right] \quad (12)$$

where the angles θ_1 and θ_2 are determined by, respectively:

$$\theta_1 = 2\text{arcsen}\left(\frac{a}{d_0}\right) \quad (13)$$

$$\theta_2 = 2\text{arcsen}\left(\frac{a}{2p(t_p)}\right) \quad (14)$$

Finally, for a cross section of RC beam, with n steel bars of intact diameter d_{0i} (with i = 0, 1, 2,…, n), the remaining steel area after subjected to pitting corrosion is:

$$A_{r,pit} = \sum_{i=1}^{n}\left[\frac{\pi d_0^2 i}{4} - A_{pit,i}(t_p)\right] \quad (15)$$

4. Proposed model for service life assessments applied to RC members

Considering the necessity to make some quantitative prediction of the durability for RC members in the design phase, Fig. 5 shows the proposed model to perform such task, in simple way, by taking account for the total time of service life. The model follows a deterministic and probabilistic approach.

For t = 0 year and x = concrete cover, i.e., at the position of the steel bar inside the concrete, the chloride concentration is equal to the inner chloride amount C_{inner} (= 0 in the most cases). In the initiation phase (blue line in Fig. 5), there is no resistance loss, R_E, due to the deterioration of the shear force, bending moment and displacement increasing, δ, because corrosion did not start.

When the chloride concentration at x = concrete cover reaches the threshold value C_{lim}, the corrosion process begins and the time of corrosion initiation t_i is achieved. In the propagation phase (red line), as the corrosion rate increases, the resistance and stiffness of the RC member decreases. Until the condition $R_E = S$ or $\delta = \delta_{lim}$ is not reached, the corroded RC member is still capable of support the external loading actions and remains safe and useful.

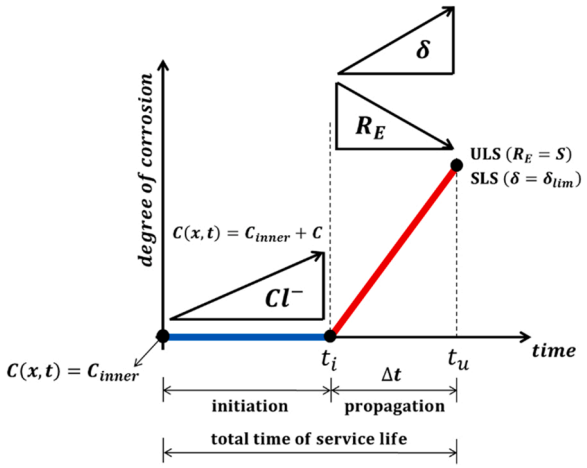

Fig. 5. Deterministic and probabilistic approach to quantitative durability prediction.

The propagation phase finishes when the adopted conditions up to the ultimate (ULS) or serviceability limit state (SLS) is reached, defining the failure time Δt. Thus, the total time of service life t_u is given by $t_u = t_i + \Delta t$.

The deterministic approach takes t_u as the final estimative for the durability of the structure. On the other hand, in the probabilistic approach, t_i and Δt are reference values, for which the probabilities of corrosion initiation and ULS or SLS achievement must be calculated, considering all the sources of uncertainties. After that, the associated risk can be assessed for those lifetimes and their probabilities. If the risks are accepted, t_i and Δt are kept and t_u represents the total time of service life. If the risks are rejected, it is necessary to adopt the acceptable risk for each phase and to find the related probabilities for corrosion initiation and ULS or SLS achievement, when the consequences of failure remain the same. The new probabilities are assessed by adopting, according to the sensibility of the random variables in the reliability analysis, new mean values for those variables that are the most important on the probability. If the new probabilities/risks of corrosion initiation and/or the structural bearing capacity are accepted, the answer of this step is the time t_i and Δt whith acceptable risks. Therefore, t_u can be calculated by the sum of t_i and Δt, to achieve the RC total time of service life, in the design phase. Further discussions can be found in the next sections of this paper.

5. Deterministic approach applied to RC beams

The isostatic RC beam subjected to g + q loadings, where q and g are the live and dead load, respectively, has been considered. The analysed cross-sections have the maximum internal efforts for bending moment $M_f = \frac{(g+q)L^2}{8}$ (at half-span cross section) and shear force $V = \frac{(g+q)L}{2}$ (at extreme cross sections called "V100″ and "V101″ in Fig. 6).

The rectangular cross-section of the beam has 20.0 × 55.0 cm with span L = 6.0 m. The adopted materials are: concrete with characteristic compressive strength, $f_{ck} = 30.0$ MPa and steel bars with characteristic tensile yield strength, $f_{yk} = 500.0$ MPa. The adopted partial safety factors for the RC beam design at ULS are 1.40 for concrete, 1.15 for steel, 1.40 for dead and live load [23]. The q and g loadings are correlated each other by the loading ratio $R = \frac{q}{(g+q)}$. The adopted dead load g is 19.71 kN/m, including self-weight of the beam, RC slab and a simple masonry wall. The RC beams were designed by considering the classical equilibrium equations of axial force (in which case is zero) and bending moment in a rectangular cross section.

Table 2 lists the amount of reinforcement and its detailing for different values of R, q and CAA, whereas Fig. 7 shows the half-span cross-section of the designed beams. The longitudinal and transversal reinforcement, in all cases, are constant along the entire beam's length.

The RC beams have been studied under vertical (case 1) and horizontal (case 2) chloride ions flux as shown in Fig. 8.

5.1. *Strength reduction in service life: chloride ions vertical flux (Case 1)*

Here a vertical chloride ions flux from the bottom to the top of the critical cross-section for bending moment (half-span cross-section) was studied (case 1 in Fig. 8).

In this case, the vertical flux of Cl^- only affects and corrodes the first longitudinal reinforcement layer (the corrosion of the bottom transversal bars is neglected in such case). Therefore, after the first layer starts the corrosion, the other layers are still intact granting some residual flexure strength for the RC beam.

Fig. 9 shows the loss of the resistant bending moment M_R for each loading ratio R in function of t_p for CAA II and CAA III, with w/c = 0.50. The dotted lines correspond to the total bending momentM_f for each R, whereas the solid lines represent the resistant bending moments M_R that decrease with the corrosion propagation.

According to Fig. 9, for both CAA II and III, the curves of the resistant bending moment are very similar for $0 < t_p \leq 15$years. It occurs, for all R, because only the neutral axis position x_{LN}, correlated to A_S losses, changes; whereas the other parameters to M_R assessment (i.e., concrete compressive strength and cross-section dimensions) stay the same.

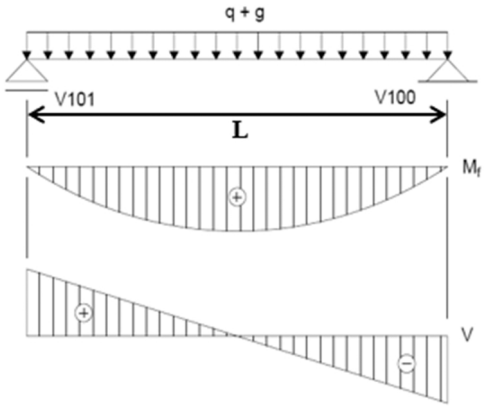

Fig. 6. Static diagrams of the analysed beam.

Table 2
Detailing of the RC beams.

CAA II: Concrete cover x = 3.0 cm			
R	**q(kN/m)**	Longitudinal reinforcement	Transversal reinforcement
0.10	2.19	3 Φ 16 mm + 1 Φ 12.5 mm = 7.25 cm^2	Φ 6.3/13 cm = 2.32 cm^2
0.20	4.93	3 Φ 16 mm + 1 Φ 16 mm = 8.0 cm^2	Φ 6.3/13 cm = 2.32 cm^2
0.30	8.45	3 Φ 16 mm + 1 Φ 16 mm + 1Φ 12.5 mm = 9.25 cm^2	Φ 6.3/13 cm = 2.32 cm^2
0.40	13.14	3 Φ 16 mm + 2 Φ 16 mm + 1 Φ 12.5 mm = 11.25 cm^2	Φ 6.3/9 cm = 2.65 cm^2
0.50	19.71	3 Φ 16 mm + 3 Φ 16 mm + 1 Φ 16 mm = 14.0 cm^2	Φ 6.3/6 cm = 4.09 cm^2
CAA III: Concrete cover x = 4.0 cm			
R	**q(kN/m)**	**Longitudinal reinforcement**	**Transversal reinforcement**
0.10	2.19	3 Φ 16 mm + 1 Φ 12.5 mm = 7.25 cm^2	Φ 6.3/13 cm = 2.32 cm^2
0.20	4.93	3 Φ 16 mm + 1 Φ 16 mm = 8.0 cm^2	Φ 6.3/13 cm = 2.32 cm^2
0.30	8.45	3 Φ 16 mm + 2 Φ 16 mm = 10.0 cm^2	Φ 6.3/13 cm = 2.32 cm^2
0.40	13.14	3 Φ 16 mm + 3 Φ 16 mm = 12.0 cm^2	Φ 6.3/9 cm = 2.65 cm^2
0.50	19.71	3 Φ 16 mm + 3 Φ 16 mm + 2 Φ 12.5 mm = 14.50 cm^2	Φ 6.3/6 cm = 4.09 cm^2

Note: Φ is the steel bar diameter ($\overline{\overline{}}$ d_0 in Fig. 4).

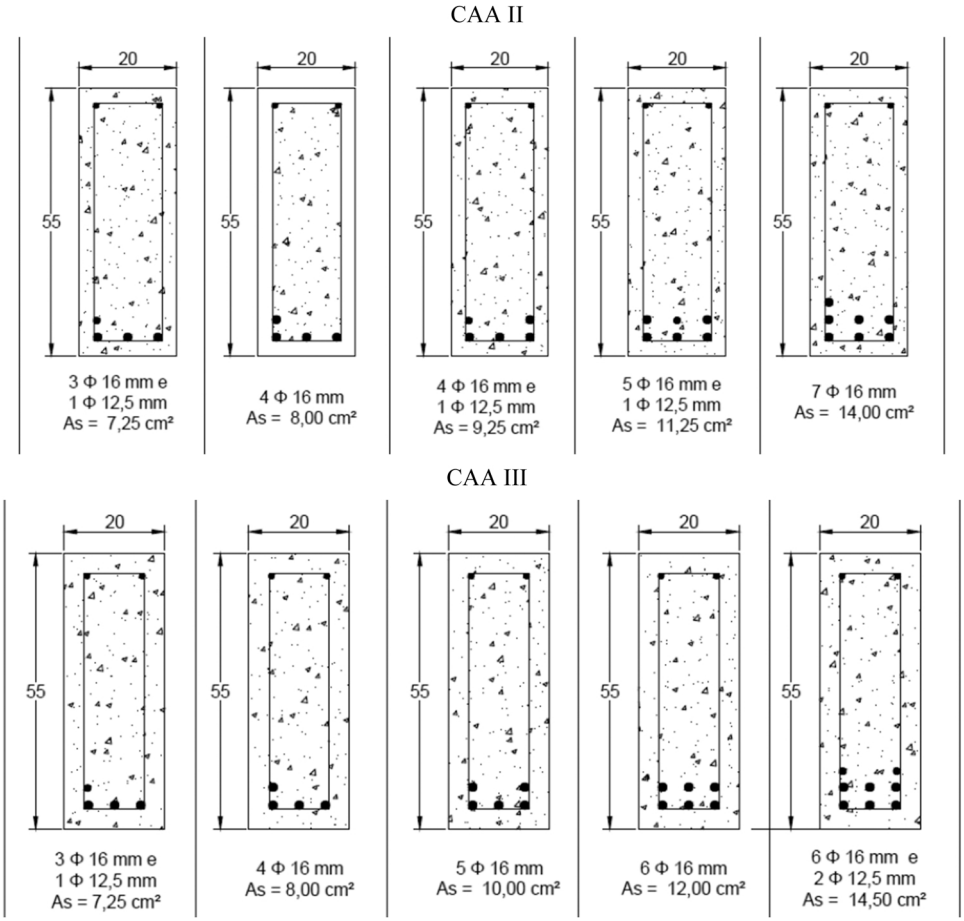

Fig. 7. Designed RC beams cross-sections.

For CAA II, after 16 years, the resistant bending moment tends to remain constant because the corrosion process did not reach the second steel layer. For CAA III, it can be observed after 25 years. Therefore, to keep some acceptable mechanical capacity for bending moment, in the corrosion propagation, and to increase the time-of-service life, it is possible to change the steel bars distribution at the cross-section, e.g., putting higher diameter bars in the second layer.

Table 3 shows the time after the corrosion initiation for CAA II and III, to reach the adopted failure condition given by $M_R = M_f$ (i.e., interception points of the M_R and M_f curves for each R in Fig. 9). The time to reach the failure condition is higher when R increases because the total bending moment also increases, which demands more reinforcement and consequently 2 or 3 steel layers in the cross-

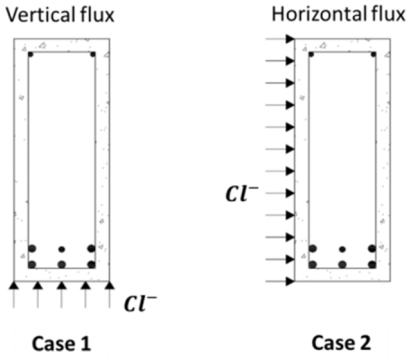

Fig. 8. Beam cross section (20.0 × 55.0 cm) subjected to vertical (case 1) and horizontal (case 2) chloride ions flux.

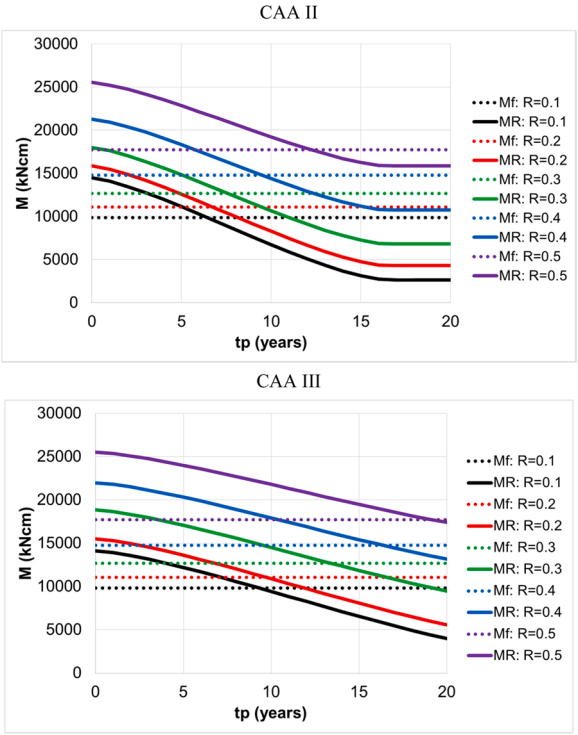

Fig. 9. Bending moment capacity loss for different R for CAA II and CAA III.

Table 3
Time to reach the failure condition.

CAA II: Concrete cover x = 3.0 cm		CAA III: Concrete cover x = 4.0 cm	
R	t (years) for $M_R = M_f$	**R**	t (years) for $M_R = M_f$
0.10	6.43	0.10	9.29
0.20	6.74	0.20	9.69
0.30	7.57	0.30	13.46
0.40	9.48	0.40	16.34
0.50	12.20	0.50	19.15

section.

Finally, t_u values applied to the RC analysed beams are shown in Table 4 and Table 5 for CAA II and III, respectively. The Δt values for CAA III are higher than those observed for CAA II because, in the first category of aggressiveness the concrete cover (i.e., 4.0 cm) is higher than in CAA II, which implies in higher values of reinforcement steel area for the same bending moment. However, when we

Table 4
Total time of service life applied to RC beams: CAA II, w/c = 0.50 and x = 3.0 cm.

R	Time of corrosion initiation t_i (years)			Δt (years)	Total time of service life t_u (years)		
	Model B	Model P	Model F		Model B	Model P	Model F
0.1	16.0	9.0	37.0	6.43	22.43	15.43	43.43
0.2				6.74	22.74	15.74	43.74
0.3				7.57	23.57	16.57	44.57
0.4				9.48	25.48	18.48	46.48
0.5				12.20	28.20	21.20	49.20

Table 5
Total time of service life applied to RC beams: CAA III, w/c = 0.50 and x = 4.0 cm.

R	Time of corrosion initiation t_i (years)			Δt (years)	Total time of service life t_u (years)		
	Model B	Model P	Model F		Model B	Model P	Model F
0.1	7.0	4.0	13.0	9.29	16.29	13.29	22.29
0.2				9.69	16.69	13.69	22.69
0.3				13.46	20.46	17.46	26.46
0.4				16.34	23.34	20.34	29.34
0.5				19.15	26.15	23.15	32.15

build the RC structure in a high aggressive environment (i.e., CAA III), the total time of service life results lesser, as expected, than in places with CAA II.

Fig. 10 shows the total time of service life t_u considering only model F for all values of R, w/c = 0.50 and CAA II and III. For concrete cover 4.0 cm in CAA III, the total time of service life is influenced almost equally by the time of corrosion initiation (i.e., 13.0 years) and failure time (i.e., mean of 13.0 years considering all R).

However, if the concrete cover increases to 4.50 cm or 5.0 cm, in such case, the total time of service life also increases, at least, 5.0 or 10.0 years, respectively. This is obtained only for the time of corrosion initiation, in which x = 4.0 cm (13.0 years) to x = 4.5 cm (18.0 years) or x = 5.0 cm (23.0 years). Moreover, if the RC beams have higher values of longitudinal reinforcement steel area, they will spend more time to reach the failure condition and, consequently, the total time of service life t_u will be higher as well.

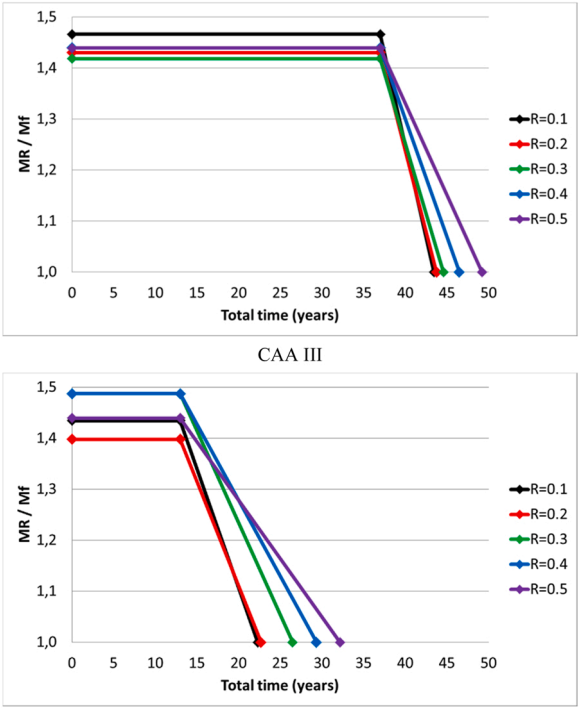

Fig. 10. Total time of service life using model F for different R applied to CAA II and CAA III.

5.2. Strength reduction in service life: chloride ions horizontal flux (Case 2)

The second analysis regards the unilateral horizontal chloride ions flux (case 2 in Fig. 8) applied on the critical cross-section for shear force (supports cross-section). In such case, the lateral flux of Cl^- only affects and corrodes one branch of the transversal reinforcement. The corrosion of the longitudinal reinforcement bars after the stirrup vertical branch is neglected in this case.

Fig. 11 shows the loss of the resistant shear force V_R for each loading ratio R in function of t_p for CAA II (x = 3.0 cm) and CAA III (x = 4.0 cm), with w/c = 0.50. The dotted lines correspond to the total shear force solicitation V for each R, whereas the solid lines represent the resistant shear force V_R that decrease with the corrosion propagation.

The curves of the V_R losses decrease up to a certain value where a constant capacity is reached. Given that corrosion affects only the left vertical bars, the degradation process of V_R tends to stabilize because of the intact right vertical branch of the stirrups and the concrete/complementary shear mechanisms contributions (sound concrete, aggregate interlock, and dowel action).

When R varies between 0.10 and 0.30, the calculated shear reinforcement is lower than the minimum stirrup amount, thus the minimum shear reinforcement ratio is adopted. For such cases, even with corrosion of the stirrups left branch, there still is a residual mechanical capacity higher than the shear force solicitation, which guarantees the resistance of the beam with no shear failure. On the other hand, for R = 0.40 and 0.50, the time until shear failure is 3.30 and 2.50 years for CAA II, 5.0 and 4.0 years for CAA III, respectively.

It is worth to mention that in real RC structures, the stirrups can be exposed and corroded without visible failure effects. Moreover, only some stirrups or part of them could be partially and/or totally deteriorated. However, several other stirrups can still resist and, in addition with sound concrete and complementary shear mechanisms [39], can maintain the shear mechanical resistance of the RC structures. To incorporate the shear reinforcement deterioration in the total time of service life t_u prediction, more complex and accurate analysis is required, with special recommendation for those that consider the chloride ions penetration in the whole structure at the same time. Thus, with some corrosion points along the stirrups (and not only in one cross section), the internal shear transference can be affected and, consequently, a shear failure scenario can be proper modelled.

6. Probabilistic approach for RC beams

6.1. Reliability theory

The reliability or probability of non-failure P_S is the complementary event of the probability of failure P_f, given by [34]:

$$P_S = 1 - P_f \tag{16}$$

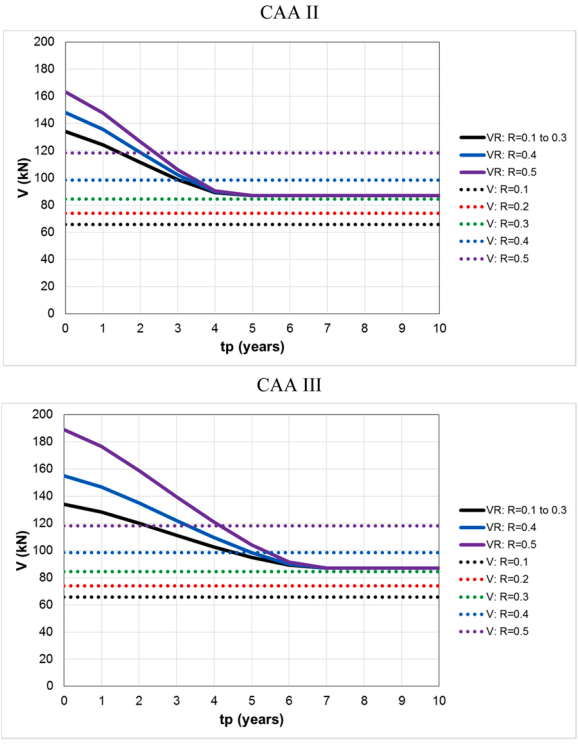

Fig. 11. Shear force capacity loss for different R for CAA II and CAA III.

The probability of failure is always associated to some undesirable scenario, in which the analysed structure is unable to fulfil a set of performance requirements along its service lifetime. Each undesirable scenario is represented by a mathematical limit state (LS) function $g_j(X,U)$ of deterministic U and random variables X sets. A particular format of the LS function is defined when g_j is equal to zero:

$$g_j(X,U) = g_j(X_1, X_2, \ldots, X_n, U_1, U_2, \ldots, U_m) = 0 \tag{17}$$

A failure event occurs when the set of random and deterministic variables lead to $g_j(X,U) \leq 0$, indicating an event in the failure domain Ω_f, whereas the condition $g_j(X,U) > 0$ represents an event in the safety domain Ω_s. Therefore, the probability of failure can be defined by the mathematical chance of occurrence of the event $g_j(X,U) \leq 0$, such as:

$$P_f = P\left[g_j(X,U) \leq 0\right] = \int_{\Omega_f} f_X(X)dx \tag{18}$$

where $f_X(X)$ corresponds to the joint probability density function of the random variables (PDF).

In the formulation of the reliability problem, there are two adopted LS functions: the first one, $j = i$, regarding to the initiation phase $g_i(X,U)$ and the second one, $j = p$, regarding to the propagation phase $g_p(X,U)$. Each of these LS functions will be described in the following specific sections.

Two reliability solution methods have been used in this paper: (i) the First Order Reliability Method (FORM) by using the reliability index β and, (ii) the Monte Carlo simulation (MCS). Both methods have already been explained in [33,34].

6.2. Probabilistic approach applied to RC beams: initiation phase

For the initiation phase, the LS function is given by:

$$g_j(X,U) = C_{lim} - C(X,U) \tag{19}$$

where C_{lim} is the limit chloride ions concentration to depassivate the steel bars; C(X,U) corresponds to the total chloride ions concentration at the steel bars-concrete interface.

Table 6 shows the used random variables indicating their mean values, standard deviations, coefficient of variations (CVs) and the adopted PDF. The criteria of the collection data is similar to [19,34].

Fig. 12 shows the evolution of the probability of corrosion initiation for different D_c models and w/c ratios (0.40 and 0.50) considering an interval of 5.0–50.0 years. The analyses were carried out by using "RelGen" software developed by the authors of this paper [46].

As expected, the differences between the curves of w/c = 0.40 and 0.50, in both CAA, for the first two models are very significant. This is because the w/c is the only or the most important parameter for the chloride diffusion assessment in these two models. On the other hand, in model F, w/c is also an important parameter, but the presence of the other random variables mitigates its direct influence on the corrosion initiation.

In order to stablish a relationship between the deterministic and probabilistic approaches, the failure (i.e. corrosion initiation) condition is always defined when $C(X,U) = C_{lim}$. Thus, in a deterministic interpretation, when the failure condition is reached, there is a 100% probability that the corrosion will start at the obtained time. However, when the uncertainties are directly and explicitly considered in a probabilistic approach, for the same time, the probability of corrosion initiation is very different, as one can see in Tables 7–8. The main question that arises from these results is: what probability of corrosion initiation must be adopted to determine

Table 6
Random variables data for the initiation phase: time of corrosion initiation prediction.

Parameter		Mean value	Unit	CV (%)	Standard deviation	PDF	Reference
C_{lim}		0.75	kg/m^3	19.0	0.14	Uniform (0.6; 0.9)	[27]
C_0		2.95 (CAA III)	kg/m^3	50.0	1.48	Log-normal	[22,27]
		1.15 (CAA II)		50.0	0.58		
D_c	Model B	23.08 (w/c = 0.4)	mm^2/year	75.0	17.31	Log-normal	[14,19,28]
		67.42 (w/c = 0.5)			50.57		
	Model P	27.55 (w/c = 0.4)	mm^2/year	75.0	20.66	Log-normal	[15,27]
		121.67 (w/c = 0.5)			91.25		
ω_e		0.60	-	33.0	0.20	Beta (3, 2)	[13]
T		25.0 (298.0)	°C (K)	30.0	7.50	Normal	Adopted
E_a		41.8 (w/c = 0.40)	kJ/mol	10.0	4.18	Normal	[6]
		44.6 (w/c = 0.50)		10.0	4.46		
		32.0 (w/c = 0.60)		8.0	2.56		
h		0.67	-	27.0	0.18	Beta (4, 2)	[13]
m		0.20	-	82.0	0.164	Beta (1, 4)	[13]
x		CAA II = 30.0	mm	50.0	15.0	Normal	[28]
		CAA III = 40.0			20.0		

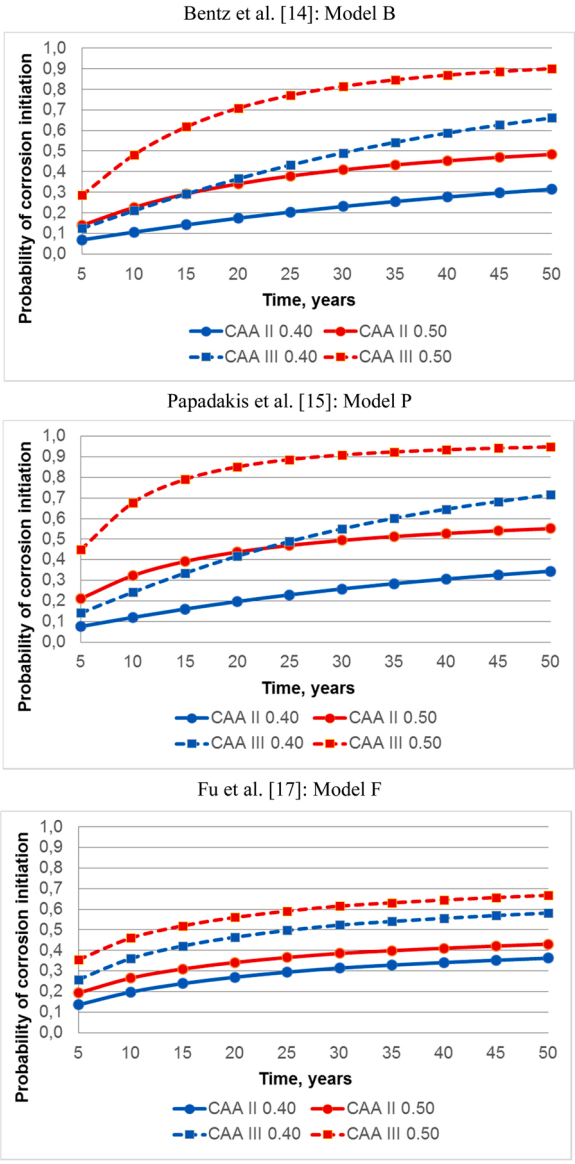

Fig. 12. Evolution of the probability of corrosion initiation for the 3 considered models.

Table 7
Deterministic and probabilistic results for CAA II and w/c = 0.50: initiation phase.

Model for $\mathbf{D_c}$	Time for $\mathbf{C(X,U) = C_{lim}}$	$\mathbf{P_{corr.initiation}^{deterministic}}$	$\mathbf{P_{corr.initiation}^{probabilistic}}$
B	16.0 years	100.0%	30.0%
P	9.0 years		30.0%
F	37.0 years		40.0%

Table 8
Deterministic and probabilistic results for CAA III and w/c = 0.50: initiation phase.

Model for $\mathbf{D_c}$	Time for $\mathbf{C(X,U) = C_{lim}}$	$\mathbf{P_{corr.initiation}^{deterministic}}$	$\mathbf{P_{corr.initiation}^{probabilistic}}$
B	7.0 years	100.0%	40.0%
P	4.0 years		40.0%
F	13.0 years		50.0%

the time to consider in the service lifetime assessment?

The answer requires a deeper discussion involving risk analysis associated to economic, social, performance, inspection and mitigation strategies applied to preserve RC structures subjected to corrosion. It also includes the definition of risk acceptance criteria, inspection plans, degradation states produced by corrosion and the costs associated to all these steps. Therefore, the time to corrosion initiation as the first term t_i of the total time of service life t_u must be adopted related to the accepted risk, weighted for all the consequences of the corrosion initiation for that RC structure. In this way, a unique value for this time t_i does not be fixed, but the risk for each category of aggressiveness and failure consequences could be.

In practical terms, as a first attempt, the deterministic time of corrosion initiation for example, that calculated according model F, is adopted; with the probability of corrosion initiation (assessed in Tables 7–8) and the evaluated consequences of reaching this state, a risk value is assessed; this risk is analysed and if is accepted, the time t_i is confirmed to estimate part of the total time of service life; if not, another value of t_i is chosen and all the steps, including probability of corrosion initiation and risk assessment, are re-evaluated until the acceptance is done.

To identify the most important random variables on the probability of corrosion initiation, Fig. 13 shows the sensitivity factors of the reliability analysis for CAA II and III. Only the models B and F have been plotted (model P has provided very similar results regarding the model B thus it was omitted). For both models, the probability of corrosion initiation values is mainly affected by x and C_0. In fact, the concrete cover depth represents the physical barrier that protects the steel bars in the RC element, whereas the surface chloride concentration reflects the aggressiveness of the environment in which this structure is placed. In case of model F, the h parameter (Eq. (6)) also affects the probability since a high humidity helps the penetration of chloride ions into concrete [34].

It is important to mention that concrete cover depth loses importance when the w/c increases for each analysed t. it occurs because the high permeability of the physical barrier (concrete cover depth) decreases its importance on the time of corrosion initiation. Therefore, adequate values of the concrete cover depth in addition with low values of w/c are essential keys to guarantee the durability of RC structures, especially because these parameters can be designed and controlled somehow by the engineer.

6.3. Probabilistic approach applied to RC beams: propagation phase

The reliability analysis has been also used to define the probability of failure for structural collapse of RC beams, to estimate the total time of service life t_u of the beams. For this, the loss of M_R and V_R has been estimated considering both case 1 and case 2 (Fig. 8).

The horizontal flux affects mostly the V_R losses, whereas the vertical flux affects the M_R losses. In both situations, the chloride ingress flux has been independent, i.e., there is no case with horizontal + vertical at the same time.

For the propagation phase, the LS functions regarding bending moments and shear force are given by:

$$g_M(X, U) = M_R - M_f - \Delta M \tag{20}$$

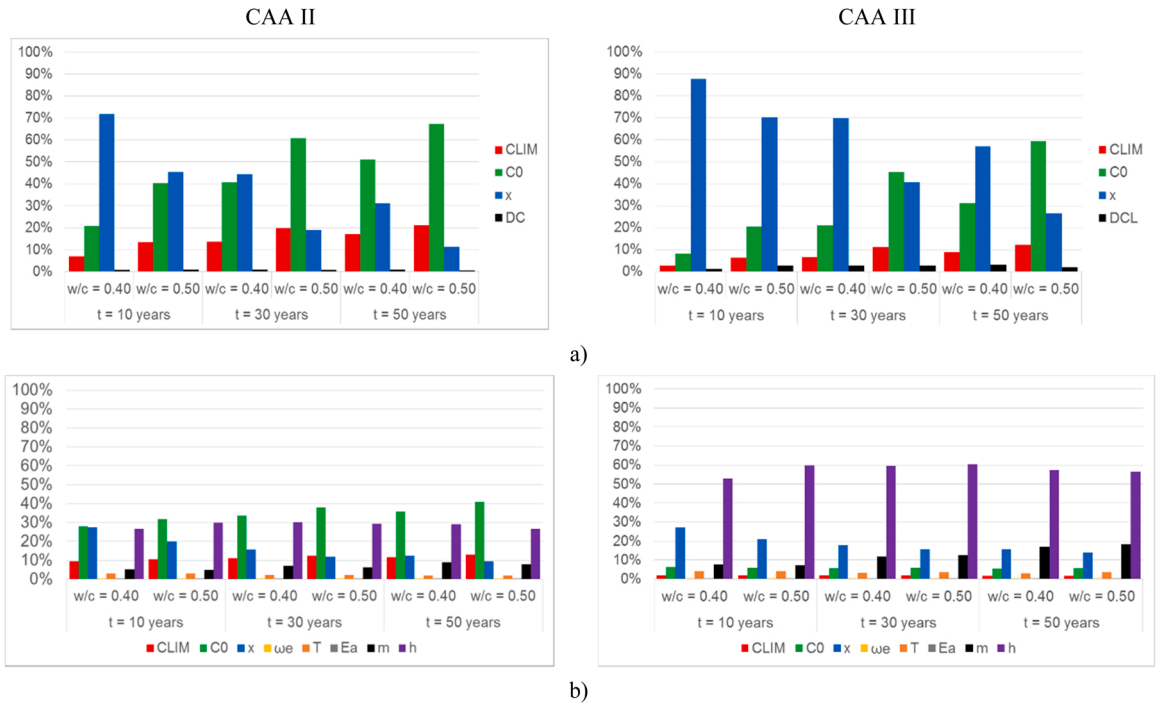

Fig. 13. Sensitivity factors for CAA II and III: a) model B and b) model F.

$$g_V(X,U) = V_R - V - \Delta V \tag{21}$$

where ΔM and ΔV are the portions of the bending moment and shear force, respectively, in which, due to the corrosion process, must be reapplied over the structure because of the longitudinal and transversal reinforcement area loss. They can be evaluated as: $\Delta M = f_{yd} \times A_{pit} \times (d - 0.4x_{LN})$ and $\Delta V = \frac{A_{pit}}{s} \times 0.9d \times f_{ywd}$, where f_{yd} and f_{ywd} are the steel design tensile yield strength for longitudinal and transversal reinforcement respectively; d is the useful beam height; s is the stirrup horizontal spacing; x_{LN} is the updated neutral axis position, which is calculated as $x_{LN} = \frac{\sigma_{sd} \times A_s}{0.68 \times b_w \times f_{cd}}$; b_w is the width of the cross section; f_{cd} corresponds to the design value of the concrete compressive strength; σ_{sd} is the updated reinforcement tensile stress.

The mathematical functions for M_R and V_R are the same given by ΔM and ΔV, respectively, except by the steel reinforcement area, which are, in both case, the original designed reinforcement area for each analysed beam.

The term A_{pit} (Eq. (10)) refers to the longitudinal and transversal reinforcement area loss as a function of the corrosion evolution.

Table 9 shows the used parameters and their statistics as random variables. All parameters have been already explained previously in the text.

Fig. 14 shows the results in terms of probability of failure for CAA II and III, w/c = 0.50 due to the losses of M_R in function of t_p (time after the corrosion initiation), considering vertical (Fig. 14a)), horizontal (Fig. 14b)) chloride ions flux and their comparison (Fig. 14c)).

The interpretation of the probability of failure P_f here is related to the collapse of the analysed isostatic RC beam, in which the condition of internal resistance (bending moment or shear force) equal to internal solicitation is reached. In general, all curves have a similar trend with a rapid increasing of P_f in the period of 5.0–15.0 years and then they stabilize.

In the case I (Fig. 14a)), especially for CAA II, the first steel layer has the most bars of the reinforcement. Thus, when the corrosion begins in a vertical chloride flux, all first bars (Fig. 7) are affected, simultaneously, by the area degradation. Consequently, high values of probability of failure are achieved because the main reinforcement layer is affected. On the other hand, for CAA III, the steel reinforcement ratio is greater than in beams detailed for CAA II. Moreover, bars with high diameters have been used, which contributed to decrease the resistance loss along time.

Another important aspect, which contributes to preserve the RC beams resistance, is the design with bars in different layers. For all cases, the constant horizontal curves indicate that the first layer is corroded, and the chloride ions penetrate in concrete between the other layers. In Fig. 14a), for R = 0.10–0.30, $P_f \approx 1.0$ at $t_p > 15.0$ years indicating the corrosion of the entire analysed layers.

In Fig. 14b), the failure scenario also corresponds to the corrosion of the first layer of the reinforcement, but it is a left lateral layer. As the lateral steel bars resemble the configuration of the vertical flux in terms of steel area, the probability of failure results is like some those obtained in the previous analysis. However, an irregular behaviour of P_f can be noted when compared to vertical flux. It is due to the type of detailing of the RC cross-section of the beam and the asymmetry that corrosion imposes over the cross-section.

Fig. 14c) compares vertical and horizontal chloride ion fluxes for R = 0.10 and 0.50. The vertical flux applies a higher probability of failure in bending moment to the RC beam when compared to the horizontal flux. This aspect confirms the previously analyses.

As the same way, the relationship for failure between the deterministic and probabilistic approaches at the propagation phase is the condition defined when $M_R = M_f$ with $\Delta M = 0$. In a deterministic interpretation, for the reached time with the abovementioned condition satisfied, the probability of collapse for the RC beam is 100.0%. But, in Fig. 14 and Tables 10–11, in the probabilistic approach, for the same reached time, the probability of failure is less than 100.0% and very different for vertical and horizontal flux.

In general, as already discussed for the time to corrosion initiation, to adopt Δt in the propagation phase to estimate the total time of service life t_u, a risk analysis must be done. It means to define risk acceptance criteria, degradation states at the corrosion evolution and all the costs associated to failure events. Therefore, here, the exact same recommendations are kept. Also, the values of probability of failure for ULS are very high in the propagation phase. When LS related to safety aspects as in ULS verification, the mean recommended targets for the probability of failure are about to $P_f \approx 10^{-4} = 0{,}01\% \leftrightarrow \beta \approx 3.80$. In fact, in Fig. 10 the Δt time in the propagation phase can be short when compared to the time of corrosion initiation. In this way, to reach acceptable values of probability of failure in the propagation phase, the considered time must be very short, perhaps even 1.0 or maximum 2.0 years after corrosion initiation. An alternative, to solve this problem, is to despise the time to reach failure in the propagation phase and to consider only the associated time to corrosion initiation as the total time of service life.

Fig. 15 shows the sensitivity factors of the bending moment of the reliability analysis for both cases with CAA III, w/c = 0.5, and R = {0.10, 0.50}. Only the most influential random variables (η, x, g, q) have been plotted here. The other used variables have a negligible influence. The results for R = 0.20–0.40 are also very similar. For the CAA II, the overall sensitivity factors are like those showed for CAA III.

It is possible to see that sensitivity factors for two cases have the same trend and values. The more influence factors are x and η. In fact, they have an inversion of relevance in t_p where x becomes the most relevant along time. Also, x cover acts in favour of the safety since for high concrete cover the structure should have more reinforcement longitudinal amount, whereas η has the opposite influence because it represents the size of the pit. The parameters g and q show a small relevance (about 5.0 – 10.0%) and they influence the probability of failure of the structure in a negative way. However, the q parameter for R = 0.50 has a great relevance between 1.0 and 2.0 years, but it strongly decreases at $t_p > 2.0$ years.

Finally, Fig. 16 shows the probability of failure curves due to V_R loss by horizontal flux for CAA II-III and w/c = 0.50. For shear force resistance loss, the P_f curves are very low. This behaviour confirms the previous results in the deterministic approach. Since the failure scenario analysed refers to the stirrup corrosion, it is noted that the resistant portion of the concrete has an important role on the shear bearing capacity of the analysed RC beam, especially for R ≤ 0.30. This can be observed by the horizontal branch of the P_f curves.

Table 9
Random variables for the propagation phase: bending moment and shear force losses prediction.

Parameter		Mean value	Unit	CV (%)	Standard deviation	PDF	Reference
f_{cd}		3.72	kN/cm^2	16.0	0.60	Normal	[29]
f_{yd} (longitudinal)		61.0	kN/cm^2	4.0	2.44	Normal	[29]
f_{ywd} (transversal)		61.0	kN/cm^2	10.0	6.10	Normal	[29]
q	R = 0.10	2.30	kN/m	25.0	0.57	Gumbel	[29]
	R = 0.20	5.17			1.29		
	R = 0.30	8.87			2.22		
	R = 0.40	13.80			3.45		
	R = 0.50	20.70			5.17		
g		19.71	kN/m	10.0	1.97	Normal	[29]
η		5.65	-	22.0	1.24	Gumbel	[30]
x		CAA II = 3.0	cm	25.0	0.75	Normal	Adopted
		CAA III = 4.0			1.0		

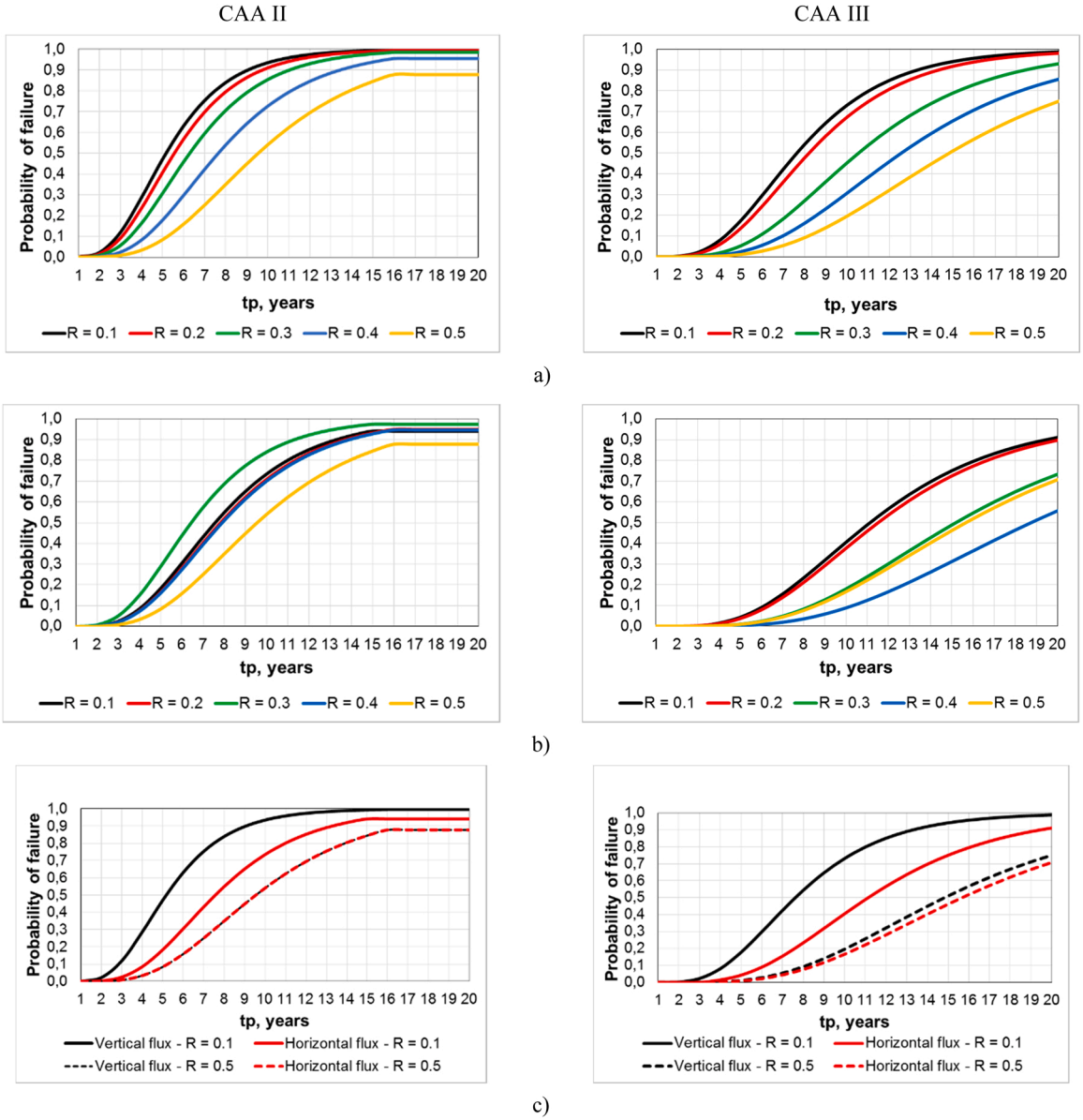

Fig. 14. Probability of failure for MR losses with CAA II, CAA III, and w/c = 0.5 for: a) case 1; b) case 2; c) comparison between case 1 and 2.

Table 10
Deterministic and probabilistic results for CAA II and w/c = 0.50: propagation phase.

R	Δt time for $M_R = M_f$	$P_{collapse}^{deterministic}$	$P_{collapse}^{probabilistic}$ Case 1	$P_{collapse}^{probabilistic}$ Case 2
0.10	6.43 years	100.0%	70.0%	35.0%
0.20	6.74 years		68.0%	34.0%
0.30	7.57 years		65.0%	65.0%
0.40	9.48 years		69.0%	66.0%
0.50	12.20 years		71.0%	72.0%

Table 11
Deterministic and probabilistic results for CAA III and w/c = 0.50: propagation phase.

R	Δt time for $M_R = M_f$	$P_{collapse}^{deterministic}$	$P_{collapse}^{probabilistic}$ Case 1	$P_{collapse}^{probabilistic}$ Case 2
0.10	9.29 years	100.0%	68.0%	34.0%
0.20	9.69 years		65.0%	35.0%
0.30	13.46 years		71.0%	40.0%
0.40	16.34 years		72.0%	38.0%
0.50	19.15 years		70.0%	67.0%

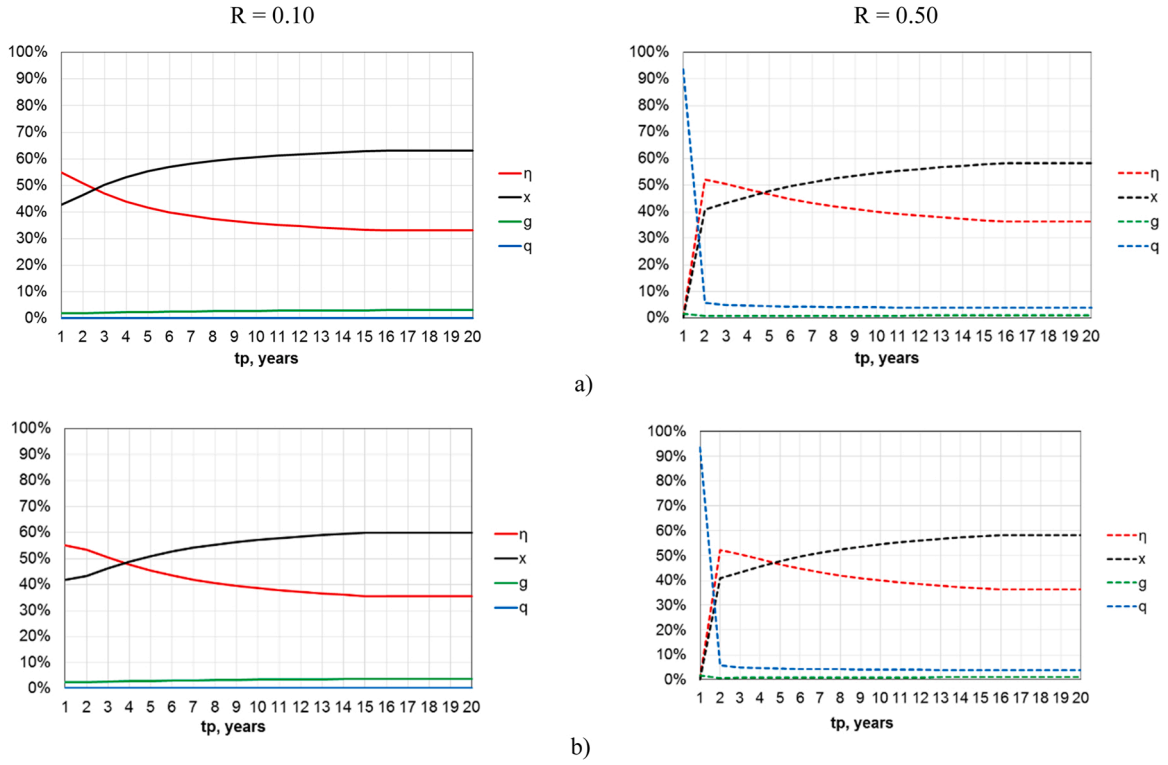

Fig. 15. Sensitivity factors for bending moment LS with CAA III and w/c = 0.5 for a) case 1 and b) case 2.

At the most cases, the necessary shear reinforcement was always given by the minimum ratio, except for R = 0.40 and 0.50.

The bending moment, when compared to shear force behaviour, has still much more influence over the safety along time in RC beams, especially because the longitudinal reinforcement has the main role on the structural safety of the beams. On the other hand, the complementary mechanisms of shear resistance (such as, aggregate interlock and dowel action) and the sound concrete play a significantly contribution in the overall structural performance of these RC structures.

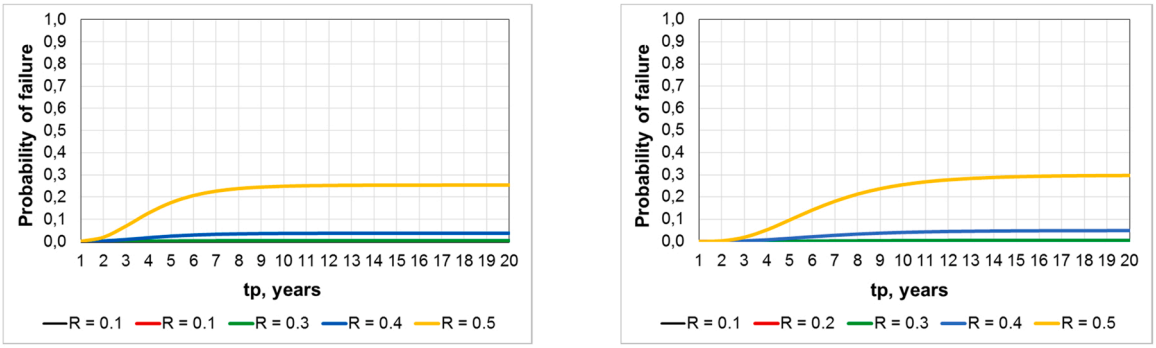

Fig. 16. Probability of failure due to VR loss (only case 2) for a) CAA II and b) CAA III.

7. Conclusion

In this paper, several aspects of corrosion in RC structures, such as time to corrosion initiation, resistance losses and total service lifetime prediction were addressed, considering deterministic and probabilistic approaches. A new simple model has been proposed and applied.

The main conclusions are:

- The diffusivity D_c was analysed considering the models B, P and F. The first two models are very simple without considering environmental parameters. The model F, which considers the temperature and humidity, provided better results, for this, its use can be recommended to achieve the time of corrosion initiation t_i.
- In the deterministic approach, the time of corrosion initiation t_i can be assessed by the comparison between C and C_{lim} values. It depends on strongly to the adopted D_c, the concrete cover, w/c ratio, C_0, and level of aggressiveness. In the probabilistic approach, it is possible to calculate the probability of corrosion initiation for each required time defined by the analyst. Thus, for each adopted time after the structure is built, e.g., 5.0 – 35.0 years, it is possible to associate the probability of the violation of the initiation corrosion condition. Moreover, considering that the consequences of corrosion in a RC structure are almost the same in terms of performance, and a certain limit state must be avoided, we can approximate the probability of corrosion initiation to the risk associated to this limit state. Therefore, to estimate t_i we can assess the probability of corrosion initiation and choose the time which will better represent the durability of the structure. The proposed approach (Fig. 5) can be used as the first approximation to the probability of corrosion initiation assessment, in the probabilistic design.
- In the propagation phase, for the standard RC beams in which the main structural behaviour is defined by the bending moment over shear force, the loss of shear force resistance could be neglected. Moreover, it can be assumed especially due to the presence of the complementary mechanisms (i.e., aggregate interlock, dowel action concrete sound) of shear resistance, which give to the RC structure other ways than the transversal reinforcement to support the shear force solicitation. Thus, in the propagation phase, the LS defined by the bending moment loss must be considered as the main ULS for the structural failure. In addition, it was shown, in Fig. 10, how much the reinforcement longitudinal details have influenced the residual bending moment resistance in the corrosion propagation phase. Larger diameters combined with multilayer positions of the longitudinal steel bars can be more effective in preserving the flexure resistant capacity of the RC beams along time when they are subjected to corrosion.
- The vertical flux has a higher probability of failure in bending moment when compared to the horizontal flux. Results show that the vertical flux reaches, at the same time, all the reinforcement bars in the first steel layer. On the other hand, the horizontal flux reaches steel bars in all the reinforcement layers, which induces some irregular and asymmetric behaviour in the bending moment capacity at the propagation phase. However, when the amount of longitudinal reinforcement is high and the bars are disposed in multiple layers, the vertical and horizontal flux can induce the same response along time, as shown Fig. 14c) for $R = 0.5$.
- The sensitivity results in Fig. 12 highlight the most important parameters: x, C_0, and h. In CAA III, h is influenced even more than the other parameters. For the propagation phase, the most important parameters are: x and η (Fig. 15). In both phases, x is the parameter which most influenced the probabilities. Its influence has always been beneficial because, in all cases, when x increased the probability of failure decreased.
- The deterministic approach for the total time of life service prediction allows to estimate each isolated time, i.e., for corrosion initiation and for mechanical failure at the propagation phase. The proposed methodology (Fig. 5) can give us, for any category of aggressiveness, material/geometric parameters and environmental conditions, a “deterministic” time for total life service. However, when the uncertainties are explicitly considered in the predictions, the probabilities of corrosion initiation and ultimate capacity are very high, with possible unacceptable values for the same deterministic total time of life service. Therefore, in such cases, the total time of service life must be adopted always in addition to the associated and acceptable risk for each phase. Moreover, as the values of probability of failure for ULSs are very high in the propagation phase the total time of service life can be achieved considering only the associated time to corrosion initiation, despising the entire propagation phase.

Declaration of Competing Interest

The authors declare that they have no known competing financial interests or personal relationships that could have appeared to influence the work reported in this paper.

Data availability

Data will be made available on request.

Acknowledgements

The authors would like to thank FAPESP (São Paulo Research Foundation), EDITAL PROPG 07/2023, for the financial support to this project.

References

[1] Pellizzer, G.P., On the numerical modelling of chloride diffusion in concrete: an approach using the boundary elements method with the application of reliability and optimization models, Doctoral Thesis, University of São Paulo (USP), São Carlos, Brazil, p. 233, 2019.
[2] Helene, P.R.L., Corrosion in reinforcement for reinforced concrete, São Paulo, Brazil, Pini/IPT 1986.
[3] Cascudo, O., Corrosion control of concrete reinforcement: inspection and electrochemical techniques, São Paulo, Brazil, Pini/Goiânia, UFG, 1997.
[4] D.V. Val, M.G. Stewart, Life-cycle cost analysis of reinforced concrete structures in marine environments, Struct. Saf. 25 (2003) 343–362.
[5] C.A. Apostolopoulos, V.G. Papadakis, Consequences of steel corrosion on the ductility properties of reinforcement bar, Constr. Build. Mater. 22 (2008) 2316–2324.
[6] C.L. Page, N.R. Short, El Tarras, A. Diffusion of chloride ions in hardened cement pastes, Cem. Concr. Res. 11 (1981) 395–406.
[7] C. Andrade, Calculation of chloride diffusion-coefficients in concrete from ionic migration measurements, Cem. Concr. Res. 23 (1993) 724–742.
[8] B. Martin-Perez, S.J. Pantazopoulou, M.D.A. Thomas, Numerical solution of mass transport equations in concrete structures, Comput. Struct. 79 (2001) 1251–1264.
[9] Mehta, P.K., Monteiro, P.J.M., Concrete: microstructure, properties and materials, São Paulo, Ibracon, 2008.
[10] S. Zhang, C. Lu, R. Li, Experimental determination of chloride penetration in cracked concrete beams, Procedia Eng. 24 (2011) 380–384.
[11] E. Bastidas-Arteaga, A. Chateauneuf, M. Sanchez-Silva, P. Bressolette, F. Schoefs, A comprehensive probabilistic model of chloride ingress in unsaturated concrete, Eng. Struct. 33 (2011) 720–730.
[12] C. Alonso, C. Andarde, M. Castellote, P. Castro, Chloride threshold values to depassivate reinforcing bars embedded in a standardized OPC mortar, Cem. Concr. Res. 30 (2000) 1047–1055.
[13] E. Zacchei, C.G. Nogueira, Chloride diffusion assessment in RC structures considering the stress-strain state effects and crack width influences, Constr. Build. Mater. 201 (2019) 100–109.
[14] D.P. Bentz, J.R. Clifton, K.A. Snyder, Predicting service life of chloride-exposed reinforced concrete, Concr. Int. 18 (1996) 42–47.
[15] V.G. Papardakis, A.P. Roumeliotis, M.N. Fardis, C.G. Vagenas, Mathematical modelling of chloride effect on concrete durability and protection measures, Concr. Repair, Rehabil. Prot. 1996 (1996) 165–174.
[16] Y. Xi, Z.P. Bazant, Modeling chloride penetration in saturated concrete, J. Mater. Civ. Eng. 11 (1999) 58–65.
[17] C. Fu, X. Jin, H. Ye, N. Jin, Theoretical and experimental investigation of loading effects on chloride diffusion in saturated concrete, J. Adv. Concr. Technol. 13 (2015) 30–43.
[18] M.P. Enright, D.M. Frangopol, Probabilistic analysis of resistance degradation of reinforced concrete bridge beams under corrosion, Eng. Struct. 20 (1998) 960–971.
[19] J. El Hassan, P. Bressolette, A. Chateauneuf, K. El Tawil, Reliability based assessment of the effect of climatic conditions on the corrosion of RC structures subject to chloride ingress, Eng. Struct. 32 (2010) 3279–3287.
[20] G.P. Pellizzer, E.D. Leonel, The cover thickness design of concrete structures subjected to chloride ingress from RBDO solution technique, IBRACON Estrut. Mater. 13 (2020), e13502.
[21] K. Tuutti, Corrosion of steel in concrete, Swedish Cement and Concrete Research Institute,, Stockholm, 1982.
[22] R.W. Mcgee, On the service life modelling of Tasmanian concrete bridges, University of Tasmania,, 2001.
[23] Brazilian Association of Technical Standards (ABNT), NBR 6118: Design of concrete structures – Procedure, Brasilia, Brazil, 2014.
[24] J.S. Kong, A.N. Ababneh, D.M. Frangopol, Y. Xi, Reliability analysis of chloride penetration in saturated concrete, Probabilistic Eng. Mech. 17 (3) (2002) 305–315.
[25] S.J. Kwon, U.J. Na, S.S. Park, S.H. Jung, Service life prediction of concrete wharves with early-aged crack: Probabilistic approach for chloride diffusion, Struct. Saf. 31 (2009) 75–83.
[26] P.Z. Bazant, L.J. Najjar, Drying of concrete as a nonlinear diffusion problem, Cem. Concr. Res. 1 (1971) 461–473.
[27] K.A.T. Vu, M.G. Stewart, Structural reliability of concrete bridges including improved chloride-induced corrosion models, Struct. Saf. 22 (2000) 313–333.
[28] C.G. Nogueira, E.D. Leonel, Probabilistic models applied to safety assessment of reinforced concrete structures subjected to chloride ingress, Eng. Fail. Anal. 31 (2013) 76–89.
[29] Santiago, W.C., Reliability-based calibration of the partial safety factors of the main Brazilian structural design standards, Doctoral Thesis, University of São Paulo (USP), São Carlos, Brazil, p. 181, 2019.
[30] M.G. Stewart, Spatial variability of pitting corrosion and its influence on structural fragility and reliability of RC beams in flexure, Struct. Saf. 26 (2004) 453–470.
[31] D.V. Val, R.E. Melchers, Reliability of deteriorating RC slab bridges, J. Struct. Eng. (ASCE) 123 (1997) 1638–1644.
[32] European Committee for Standardization (CEN), Eurocode 2 – Design of concrete structures – Part 1–1: General rules and rules for buildings, EN 1992–1-1:2004, Brussel, Belgium, 2004.
[33] Cheung, A.B., Stochastic model of stored product pressures to estimate the structural reliability of slender silos, Doctoral Thesis, University of São Paulo (USP), São Carlos, Brazil, p. 305, 2007.
[34] E. Zacchei, C.G. Nogueira, 2D/3D numerical analyses of corrosion initiation in RC structures accounting fluctuation of chloride ions by external actions, KSCE J. Eng. 2021 (2021) 1–16.
[35] E. Bastidas-Arteaga, P. Bressolette, A. Chateauneuf, M. Sánchez-Silva, Probabilistic lifetime assessment of RC structures under coupled corrosion-fatigue deterioration processes, Struct. Saf. 31 (2009) 84–96.
[36] A. Farahani, H. Taghaddos, M. Shekarchi, Prediction of long-term chloride diffusion in sílica fume concrete in a marine environment, Cem. Concr. Compos. 59 (2015) 10–17.
[37] J. Lizarazo-Marriaga, C. Higuera, I. Guzmán, L. Fonseca, Probabilistic modelling to predict fly-ash concrete corrosion initiation, J. Build. Eng. 30 (2020) 1–8.

[38] J.C. Guerra, A. Castañeda, F. Corvo, J.J. Howland, J. Rodriguez, Atmospheric corrosion of low carbon steel in a coastal zone of Ecuador: Anomalous behaviour of chloride deposition versus distance from the sea, Mater. Corros. 70 (2019) 444–460.
[39] C.H. Nogueira, W.S. Venturini, H.B. Coda, Material and geometric nonlinear analysis of reinforced concrete frame structures considering the influence of shear strength complementary mechanisms, Lat. Am. J. Solids Struct. 10 (2013) 953–980.
[40] E. Zacchei, C.G. Nogueira, Calibration of boundary conditions correlated to the diffusivity of chloride ions: an accurate study for random diffusivity, Cem. Concr. Compos. 2022 (2022) 1–14.
[41] Y.C. Ou, H.D. Fan, N.D. Nguyen, Long-term seismic performance of reinforced concrete bridges under steel reinforcement corrosion due to chloride attack, Earthq. Eng. Struct. Dyn. 42 (2013) 2113–2127.
[42] J. Liu, G. Ou, Q. Qiu, X. Chen, J. Hong, F. Xing, Chloride transport and microstructure of concrete with/without fly ash under atmospheric chloride condition, Constr. Build. Mater. 146 (2017) 493–501.
[43] P. Helene, Contribution on the study for corrosion bars in RC structures, São Paulo: USP, thesis for Associate Professor, Polytech. Sch. São Paulo Univ. (1993) 271.
[44] K. Dinh, T. Zayed, S. Moufti, A. Shami, A. Jabri, M. Abouhamad, T. Dawood, Clustering-based threshold model for condition assessment of concrete bridge decks with ground-penetrating radar, Transp. Res. Rec.: J. Transp. Res. Board 2522 (2015) 81–89.
[45] E. Zacchei, E. Bastidas-Arteaga, Multifactorial chloride ingress model for reinforced concrete structures subjected to unsaturated conditions, Buildings (2022) 1–23.
[46] Nogueira, C.G., Development of mechanical, reliability and optimization models for application in reinforced concrete structures. 345 p., Ph.D Thesis, School of Engineering of São Carlos, University of São Paulo, São Carlos, 2010 (in Portuguese).
[47] C. Turco, M.F. Funari, E. Teixeira, R. Mateus, Artificial neural networks to predict the mechanical properties of natural fibre-reinforced compressed earth blocks (CEBs), Fibers 9 (2021) 1–21.
[48] I. Afshoon, M. Miri, S.R. Mousavi, Combining Kriging meta models with U-function and K-means clustering for prediction of fracture energy of concrete, J. Build. Eng. 35 (2021) 1–16.
[49] L. Chen, W. Shan, P. Liu, Identification of concrete aggregates using K-means clustering and level set method, Structures 34 (2021) 2069–2076.
[50] S. Tayfur, N. Alver, S. Abdi, S. Saatci, A. Ghiami, Characterization of concrete matrix/steel fiber de-bonding in an SFRC beam: principal component analysis and k-mean algorithm for clustering AE data, Eng. Fract. Mech. 194 (2018) 73–85.
[51] Y. Ma, Z. Guo, L. Wang, J. Zhang, Probabilistic life prediction for reinforced concrete structures subjected to seasonal corrosion-fatigue damage, J. Struct. Eng. 146 (7) (2020), 04020117.
[52] Y. Ma, Y. He, Z. Guo, L. Wang, J. Zhang, D. Lee, Corrosion fatigue crack growth prediction of bridge suspender wires using Bayesian gaussian process, Int. J. Fatigue 168 (2023) 1–14.
[53] X.H. Wang, E. Bastidas-Arteaga, Y. Gao, Probabilistic analysis of chloride penetration in reinforced concrete subjected to pre-exposure static and fatigue loading and wetting-drying cycles, Eng. Fail. Anal. 84 (2018) 205–2019.
[54] S. Mahboub, M. Kioumarsi, Damage assessment of RC bridges considering joint impact of corrosion and seismic loads: a systematic literature review, Constr. Build. Mater. 295 (2021) 1–12.
[55] S. Hu, Z. Wang, Y. Guo, G. Xiao, Life-cycle seismic fragility assessment of existing RC bridges subjected to chloride-induced corrosion in marine environment, Adv. Civ. Eng. 2021 (2021) 1–18.
[56] R. Wang, S. Lin, On the effect of pit shape on pitted plates, Part I: tensile behavior due to artificial corrosion pits, Ocean Eng. 236 (2021) 1–13.
[57] T. Lin, J. Li, J. Liu, Analysis of time-dependent seismic fragility of the offshore bridge under the action of scour and chloride ion corrosion, Structures 28 (2020) 1–17.